Land Subsidence, Associated Hazards and the Role of Natural Resources Development
(Proceedings of EISOLS 2010, Querétaro, Mexico, 17–22 October 2010). IAHS Publ. 339, 2010.

Implications of ground-deformation measurements across earth fissures in subsidence areas in the southwestern USA

T. L. HOLZER
United States Geological Survey, 345 Middlefield Road, MS977, Menlo Park, California 94025, United States
tholzer@usgs.gov

Abstract Ground deformation was monitored at earth fissures in areas of land subsidence induced by groundwater extraction in the southwestern United States. The ground deformation is consistent with the mechanism that fissures are caused by horizontal strains generated by bending of overburden in response to localized differential compaction. Subsidence profiles indicated that localized differential subsidence occurred across the fissures and that maximum convex-upward curvature was at the fissure. The overall shape of the profile stayed similar with time, and maximum curvature remained stationary at the fissure. Horizontal displacements were largest near the fissure, and generally were small to negligible away from the fissure. Maximum tensile horizontal strains were at the fissure and coincided with maximum curvature in the subsidence profiles. Horizontal tensile strain continued to accumulate at fissures after they formed with rates of opening ranging from 30 to 120 microstrain/year at fissures in Arizona.

Key words subsidence; earth fissure; ground deformation; geodesy; monitoring; creep; groundwater; USA

INTRODUCTION

Earth fissures, long tension cracks with negligible vertical offset are common in subsiding areas in the southwestern United States where groundwater has been withdrawn from unconsolidated sedimentary aquifer systems (Holzer, 1984). These fissures pose a significant hazard because they frequently are eroded by storm runoff into metre-wide and decametre-deep gullies. Earth fissures also can divert large volumes of surface runoff and may affect groundwater quality. The impressive surface appearance of many fissures is further enhanced by their decametre to kilometre lengths. Earth fissures that are associated with land subsidence caused by groundwater withdrawal should not be confused with similar appearing large tensile ground cracks that are caused by either hydrocompaction (Lofgren, 1969) or desiccation (Neal *et al.*, 1968).

Several mechanisms have been proposed to explain the origin of the horizontal strains that cause earth fissures: (1) bending caused by localized differential subsidence, (2) regional differential subsidence, and (3) horizontal deformation within the compacting portion of the aquifer system.

Bending caused by localized differential subsidence was originally proposed by Feth (1951) to explain an earth fissure in 1949 in south-central Arizona. He speculated that it was caused by tensile strains generated by locally varying subsidence. He attributed the differential subsidence to local variations in aquifer thickness. The 1949 fissure continued to evolve, however, and in 1961 vertical offset was reported across it (Peterson, 1962). The surface scarp ultimately grew to an approximate length of 15.8 km and height of 0.6 m (Holzer *et al.*, 1978). Because the surface expression and morphology of the scarp were similar to surface faults that had been reported in other areas of land subsidence (e.g. Holzer, 1984), Holzer *et al.* (1978) formally named the feature the Picacho Fault. Subsurface exploration revealed that the Picacho Fault is the surface expression of a pre-existing tectonic fault that is a partial barrier to groundwater flow in the alluvium (Holzer, 1978; Pankratz *et al.*, 1978). Feth's (1951) proposed mechanism for fissures, however, was corroborated by Jachens & Holzer (1982) for a complex fissure system in alluvium on the east side of the Casa Grande Mountains in south-central Arizona. Their field investigation confirmed that fissures formed at locations where the aquifer system thinned because of buried topographic relief of the crystalline bedrock surface underlying the aquifer system. Topographic profiles across fissures on the undisturbed desert floor indicated differential subsidence had occurred that was proportional to aquifer thickness. Modelling of the bending process indicated tensile strains at failure ranged from 200 to 2000 microstrain.

Rotation of rigid slabs of overburden in response to regional subsidence was proposed by Bouwer (1977) as the cause of earth fissures. By Bouwer's (1977) mechanism, earth fissures should form around the margins of subsidence bowls and be oriented orthogonal to regional subsidence gradients.

Horizontal deformation within the compacting portion of the aquifer system was first proposed by Lofgren (1971). He attributed surficial horizontal displacements in subsidence areas to deep seated deformation caused by horizontal seepage forces. He hypothesized that the deformation was capable of causing earth fissures (Lofgren, 1978). Lofgren's conceptual model was formalized by Sheng *et al.* (2003), who concluded that formation of earth fissures was controlled by a complex combination of aquifer deformation at depth, pre-existing subsurface structure, and the *in situ* stress field. They hypothesized that fissures form in tensile zones that are created at depth. Fissures form in the tensile zones where sediment is brittle and susceptible to tensile failure.

The purpose of this manuscript is to present observations of ground deformation across earth fissures in subsiding areas in Arizona, California, and Nevada in the southwestern United States (Fig. 1). These observations can be used to evaluate proposed mechanisms of formation for earth fissures. Understanding of mechanism also is useful for predicting where future fissures may form (Holzer, 2000).

Fig. 1 Map of major subsidence areas in the western United States and earth fissure monitoring areas. A is Picacho Basin, B is Las Vegas Valley, Nevada, and C is Fremont Valley, California.

METHODOLOGY

Ground deformation was monitored with bench-mark arrays that were established orthogonally to each fissure. Arrays varied from multiple bench marks to bench-mark pairs. Distances between bench marks in the arrays that consisted of multiple bench marks were variable, and typically increased with distance from the earth fissure. Bench-mark pairs were 30 m apart. Ground deformation was computed based on comparisons of repeated precise geodetic surveys of the

bench marks. Both vertical and horizontal positions of bench marks were measured. Where feasible, each array included a bench mark established on nearby bedrock outcrops. This enabled computations of absolute displacements. Some fissures were too far from bedrock outcrops to justify labour-intensive levelling, and only relative displacements could be computed for these arrays.

Vertical positions of bench marks were measured by first-order levelling using a precision level and invar survey rods. Levelling was performed to first-order, class 1 standards. Such levelling has a nominal accuracy in millimetres of $1.5K^{½}$, where K is distance in kilometres between bench marks (Federal Geodetic Control Committee, 1974). Horizontal positions of bench marks were measured with a Hewlett-Packard 3805A electronic distance meter (EDM). Slope distances were measured with the EDM, and were corrected to horizontal distances based on elevations measured in the level surveys. Repeated surveys of a stable bench-mark array in Menlo Park, California, indicated that the EDM had a precision (one standard deviation) of ±1.8 mm at 202 m and ±1.2 mm at 23 m. Horizontal positions of closely spaced (=30 m) bench marks that spanned fissures were also measured with a calibrated narrow steel ribbon tape. Tape measurements were made under a constant tension and were temperature corrected. Such taping has an estimated accuracy of ±2 mm for 30-m distances (Lufkin, 1972).

GROUND DEFORMATION OBSERVATIONS

Observations of ground deformation in three study areas, Picacho Basin, Arizona, Las Vegas Valley, Nevada, and Fremont Valley, California, are presented here (Fig. 1). During the period of monitoring, 1976 to 1989, all three areas experienced water-level declines caused by groundwater extraction and subsided due to aquifer system compaction. Picacho Basin received the greatest scrutiny of the three areas because it was an agricultural area with easy access and earth fissures were widespread. Monitoring in Las Vegas Valley was particularly challenging because the urban setting was not conducive to the establishment and preservation of bench marks.

Picacho Basin, south-central Arizona

The Picacho Basin is a deep alluvial sedimentary basin southeast of Phoenix, Arizona. The shallow unconsolidated sediments in the basin constitute a major aquifer system. Water-level declines, which locally exceeded 100 m, began in approximately 1940 after the introduction of the turbine pump. Subsidence locally exceeds 2.9 m (Holzer *et al.*, 1978). A 1200-km^2 area in the basin has subsided by more than 30 cm in response to the water-level declines (Fig. 2). Earth fissures are widespread within the basin (Schumann, 1974).

Monitoring of earth fissures was conducted at eight sites in the Picacho Basin (Fig. 2). Most of the sites consisted of single curvilinear fissures, but site 5 covered a complex system of fissures. Profiles are presented here for four sites. Creep histories, based on repeated measurement of the spacing of closely spaced bench marks spanning eight fissures are presented too.

Figure 3 shows profiles of subsidence, total displacements, and horizontal strains at sites 6 and 7 in the northern Picacho Basin. Fissures at both sites were simple long curvilinear ground failures. The bench-mark arrays were originally established at the ends of newly formed fissures in anticipation that the fissures would grow in length and propagate between the bench marks, which they did within a year of the establishment of the arrays in 1976. The arrays initially consisted of two bench marks that were 30 m apart. Each array was expanded with additional bench marks a couple of years later after the fissure propagated through the initial bench-mark pair. Both arrays, when completed, extended to nearby bedrock.

Earth fissures in both subsidence profiles are located at points of maximum convex-upward curvature. The maximum curvature in each profile remained stationary at the fissure over the 6- to 7-year monitoring periods. Total displacements indicate horizontal displacements are largest near the fissure, and decrease basinward (direction of increasing subsidence). Horizontal strains computed from the horizontal displacements are tensile and largest at the fissure.

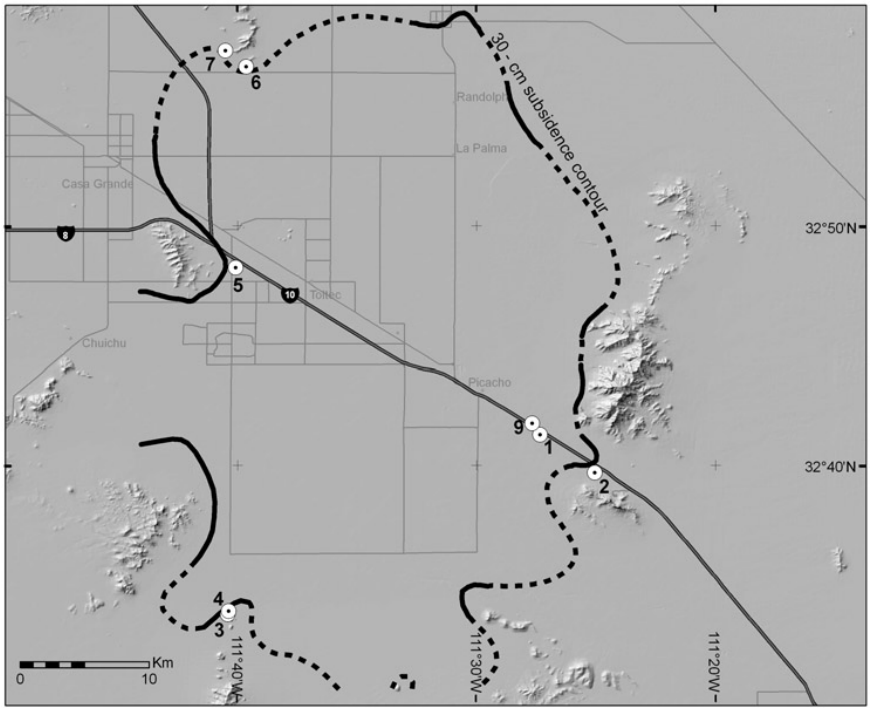

Fig. 2 Map of Picacho Basin, Arizona, and ground-failure monitoring sites. Contour outlines area where land subsidence has exceeded 30 cm. Line is solid where subsidence is confirmed by geodetic surveys, and dashed where inferred.

A profile across the first reported earth fissure in the Picacho Basin is shown in Fig. 4. The fissure formed in 1927 (Leonard, 1929), and until 1949 was the only documented fissure in the basin. The 1949 fissure reported by Feth (1951) was assumed for many years to be a re-activation of the 1927 fissure. Holzer *et al.* (1978), however, demonstrated that the 1927 fissure was located 0.87 km northwest of the 1949 fissure. Inspection of the 1927 fissure in the 1970s by the author indicated it was inactive. It was essentially filled in with sediment and barely discernible on modern aerial photographs. The 1980–1985 profiles in Fig. 4(a), which show absolute subsidence, did not detect differential ground deformation across the fissure. Subsidence was uniform across the fissure, and no differential horizontal displacements (or strain) were observed from 1980 to 1985 (Fig. 4).

Figure 5 is a profile that crosses a complex system of earth fissures in alluvium on the east side of the Casa Grande Mountains. Subsurface conditions beneath the fissure system were studied by Jachens & Holzer (1982). Ground deformation was monitored across the northern part of the fissure system. The subsidence profile reveals differential subsidence was ongoing across the eastern fissure, and that the annual accumulation of horizontal strain across the fissure was 140 microstrain. The subsurface investigation by Jachens & Holzer (1982) indicates that the fissure overlies a buried bedrock ridge at the base of the aquifer system, and the differential subsidence is attributable to variability in aquifer system thickness. Although the centre of the regional subsidence bowl is located several kilometres to the east, the total displacement vectors indicate that the ground on the western side of the ridge is moving westward towards the Casa Grande Mountains, away from the centre of the bowl.

Time histories of changes in distance between bench marks that spanned eight monitored earth fissures are shown in Fig. 6. The histories are based on taping of bench marks that were 30 m apart. The histories indicate that extension across fissures continued after the fissures formed. Long-term creep rates vary from fissure to fissure. The highest rate was measured at site 1, which continued to extend at a rate of 120 microstrain/year (3.5 mm/year). No creep was measured at site 9, which straddled the 1927 fissure.

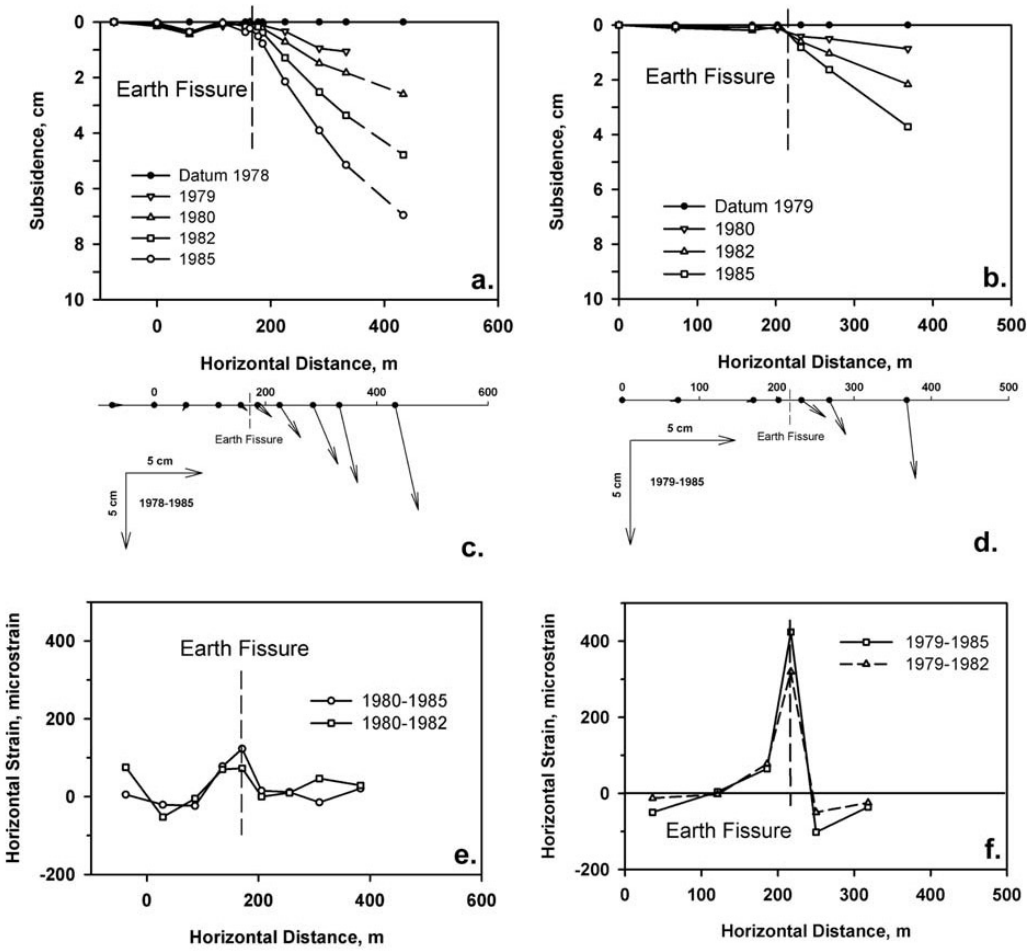

Fig. 3 Ground deformation at sites 6 (a, c, and e) and 7 (b, d, and f), northern Picacho Basin, Arizona. Positive horizontal strain in e and f are tensile.

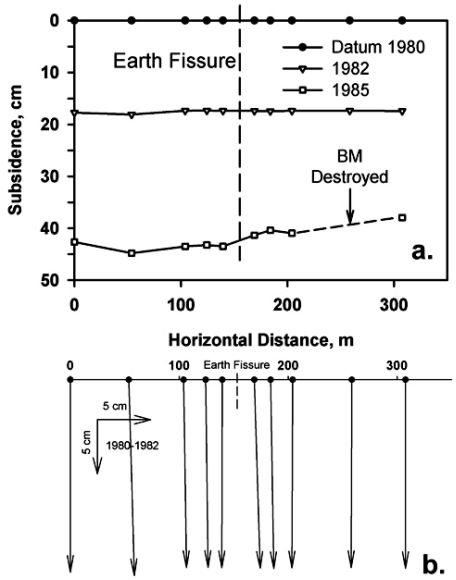

Fig. 4 Ground deformation at site 2, Picacho Basin, Arizona. Earth fissure formed in 1927 (Leonard, 1929).

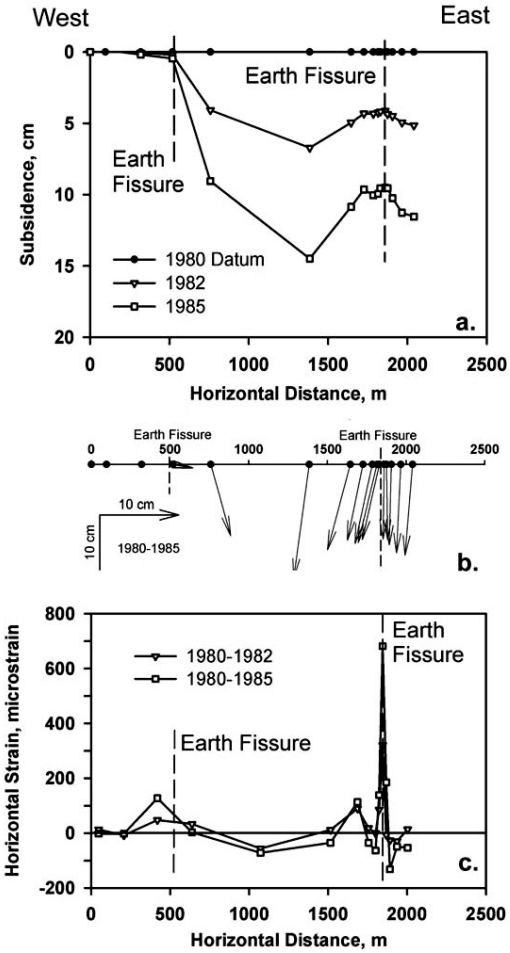

Fig. 5 Ground deformation at site 5, east side of Casa Grande Mountains, Picacho Basin Arizona. Positive horizontal strain in c is tensile.

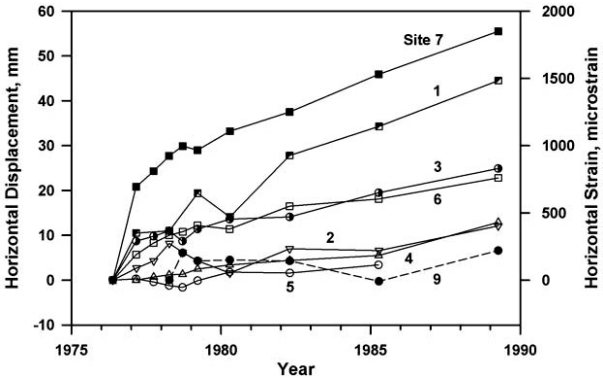

Fig. 6 Time histories of relative displacements of bench marks 30-m apart that span earth fissures in Picacho Basin, Arizona. Monitor sites are show by number in Fig. 2.

Las Vegas Valley, Nevada

Las Vegas Valley is underlain by a complex sequence of faulted alluvial sediments. These sediments have provided groundwater to the valley since 1907, and this has lead to almost

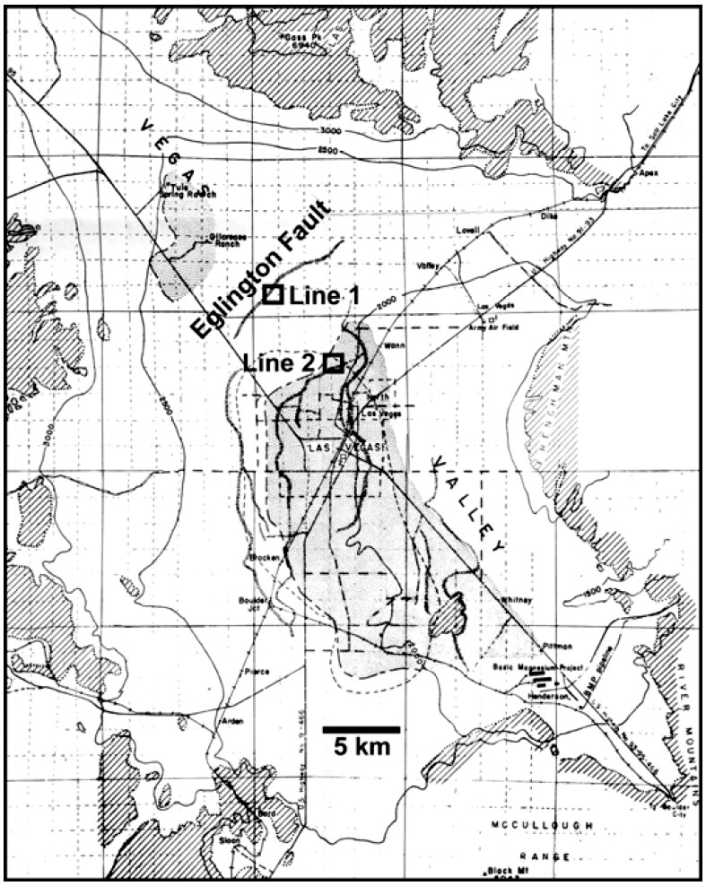

Fig. 7 Map of Las Vegas Valley (from Maxey & Jameson, 1948).

continuous water-level declines. Approximately 120 km^2 of land has subsided more than 30 cm. Maximum subsidence is more than 1.5 m (Galloway *et al.*, 1999).

Two sites were briefly monitored in Las Vegas Valley. Monitoring ended when the bench-mark arrays were destroyed by urban development. Locations of the two monitor sites are shown in Fig. 7. Line 1 was on the downthrown side of the pre-existing fault scarp, the Eglington Fault, and line 2 was on the upthrown side of a pre-existing, but unnamed, fault scarp. Both arrays were approximately 300-m long and were not referenced to a locally stable bedrock bench mark. The profiles reveal that the earth fissures are coincident with locations of maximum convex upward curvature in the subsidence profiles (Fig. 8). Horizontal displacements produced tensile strains at both fissures, although the computed strains for line 1 are ambiguous. Peak tensile strain from 1980 to 1982 at the fissure crossed by line 2 was 250 microstrain.

Fremont Valley, California

Fremont Valley is a tectonic pull-apart basin formed between left-stepping strands of the active Garlock Fault, which is a major tectonic feature in southern California (Davis & Burchfiel, 1973). Pampeyan *et al.* (1988) provide an in depth review of ground failure in Fremont Valley and its history. Groundwater levels declined locally as much as 88 m from 1954 to 1980, and regional land subsidence was documented, principally along the valley margin. Earth fissures and surface faulting were extensive in the area of groundwater level decline. Modern ground failure in Fremont Valley was first noted in August 1971, and consisted of open cracks along and on trend with Holocene fault scarps.

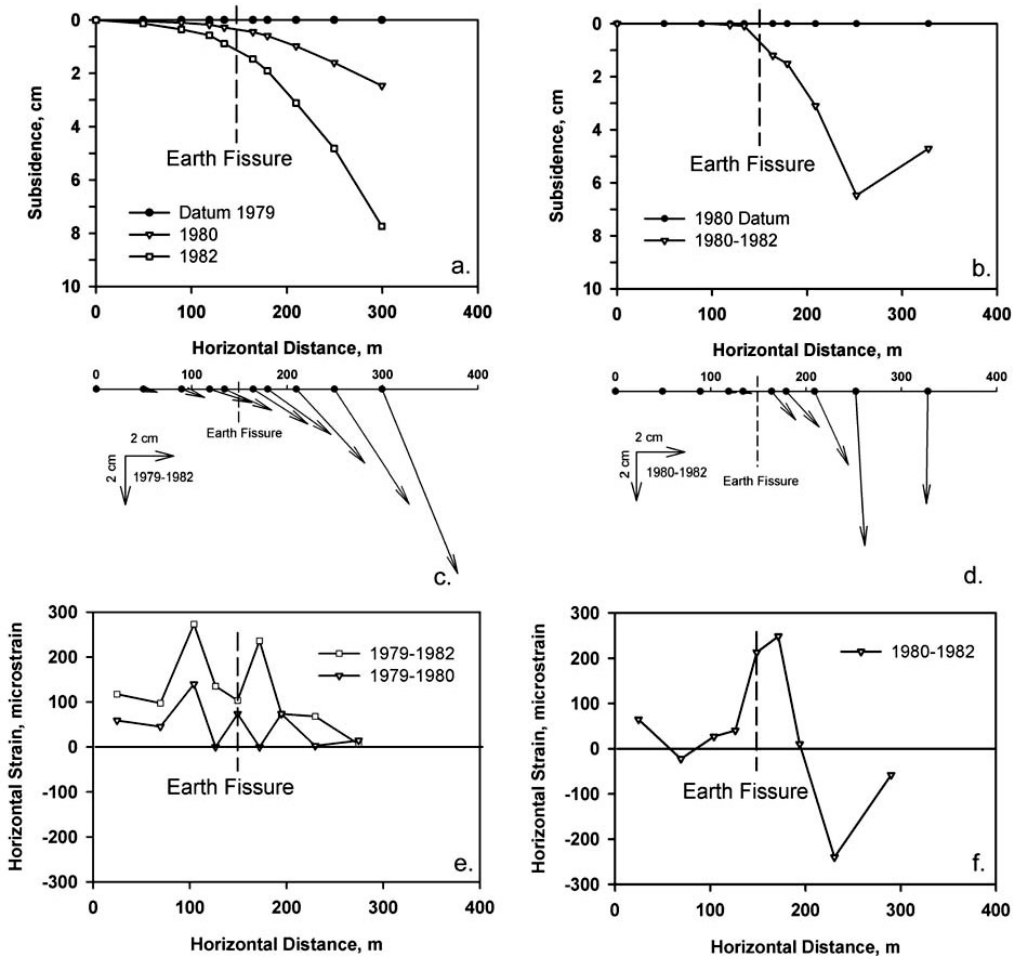

Fig. 8 Ground deformation at lines 1 (a, c, and e) and 2 (b, d, and f), Las Vegas Valley, Nevada. Positive horizontal strain in e and f are tensile.

Although Pampeyan *et al.* (1988) mapped extensive modern ground failures in Fremont Valley, only one earth fissure in the southern part of the valley was monitored (Fig. 9). Other monitored failures consisted of modern surface faulting.

Ground deformation near the earth fissure is shown in Fig. 10. The fissure occurred along a 2-m high Holocene fault scarp. The 300-m array was not referenced to a locally stable bench mark on bedrock. Displacements as shown are relative to the upthrown side of the fault scarp. Approximately 14 cm of differential subsidence occurred across the fissure from 1978 to 1985. Horizontal displacements on the downthrown side of the scarp increased from 5.7 to 10.3 cm with distance from the scarp. Differential horizontal displacements from 1978 to 1985 caused a horizontal tensile strain at the fissure of 2750 microstrain. This yields a rate of opening of 400 microstrain/year. Although not shown here, differential subsidence across the fissure decreased seasonally during periods of water level recoveries (see Holzer & Pampeyan, 1981, Fig. 3f). This suggests that some of the annual deformation was elastic and recoverable.

DISCUSSION

All of the subsidence profiles spanning the earth fissures indicate that localized differential subsidence is occurring across newly formed and active fissures. The maximum curvature in each

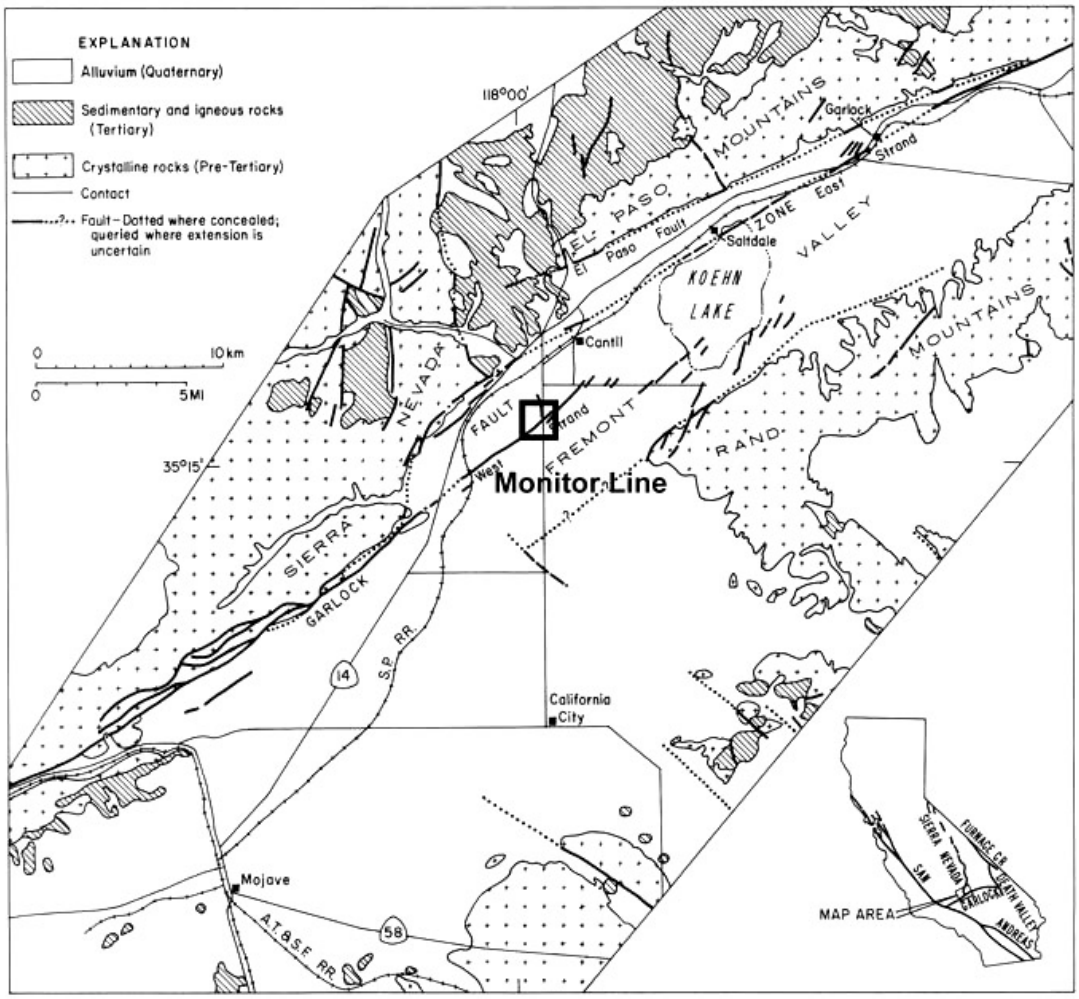

Fig. 9 Map of Fremont Valley with monitor site (from Pampeyan *et al.*, 1988).

subsidence profile is at the fissure and convex upward. The overall shape of the profile stays similar over time with maximum curvature remaining at the fissure. Horizontal displacements are largest near the fissure. In general, horizontal displacements are small to negligible away from the fissure. Variation of horizontal displacements in the profiles indicates tensile horizontal strains are at a maximum at the fissure. Maximum horizontal strain is coincident with the maximum curvature in the subsidence profiles.

The deformation fields that were observed across the earth fissures in the southwestern United States are most consistent with the mechanism for fissure formation that consists of bending caused by localized differential subsidence (Feth, 1951). This mechanism was analysed by Lee & Shen (1969) and used to predict tensile cracking in earth dams subjected to differential settlements. They showed that local differential subsidence can cause differential horizontal displacements and large tensile strains. Modelling and laboratory analyses indicated that the tensile horizontal strains are caused by simple bending of the overburden. They also demonstrated that peak tensile strains coincide with the locations of maximum convex-upward curvature in subsidence profiles as was observed here. The monitoring observations reported here are not consistent with either regional differential subsidence (Bouwer, 1977) or horizontal deformation within the compacting portion of the aquifer system (Sheng *et al.*, 2003). Neither of these mechanisms requires local differential subsidence across the earth fissure as was observed.

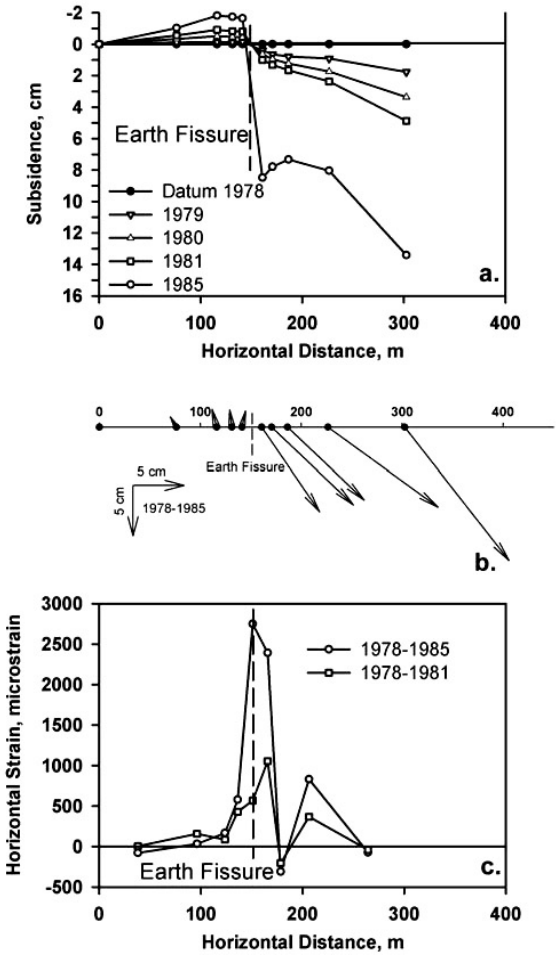

Fig. 10 Ground deformation, Fremont Valley, California. Positive horizontal strain in c is tensile.

Continued accumulation of horizontal tensile strain after fissures formed is an interesting aspect of monitoring the bench-mark pairs that spanned the fissures in Arizona. Rates of opening or creep ranged from 30–120 microstrain/year (0.9 to 3.5 mm/year). Observation of creep across earth fissures may explain why some fissures re-activate after periods of apparent dormancy and infilling with sediment. The observation of ongoing differential subsidence across fissures after they have formed is the probable explanation of this creep-like behaviour. The observation of creep suggests that a visually dormant fissure may continue to pose a displacement hazard after the fissure has formed. Fissures, however, presumably can become dormant when differential compaction ceases. This could occur in situations where groundwater levels stabilize or recover, or where a declining water table falls below the zone that is differentially compacting. The 1927 Arizona fissure may be an example of this phenomenon.

REFERENCES

Bouwer, H. (1977) Land subsidence and cracking due to groundwater depletion. *Ground Water* **15**(5), 358–364.

Davis, G. A. & Burchfiel, B. C. (1973) Garlock fault, an intracontinental transform feature, southern California. *Bull. Geol. Soc. Am.* **84**, 1407–1422.

Federal Geodetic Control Committee (1974) Classification, standards of accuracy, and general specifications of geodetic control surveys. National Oceanic and Atmospheric Administration, Washington, D.C.

Feth, J. H. (1951) Structural reconnaissance of the Red Rock Quadrangle, Arizona. *US Geological Survey Open-file Report 51-199*, p.32.

Galloway, D., Jones, D. R. & Ingebritsen, S. E. (1999) Land subsidence in the United States. *US Geological Survey Circular 1182*, p. 175.

Holzer, T. L. (1978) Results and interpretation of exploratory drilling near the Picacho fault, south-central Arizona. *US Geological Survey Open-file Report 78-1016*, p. 17.

Holzer, T. L. (1984) Ground failure induced by ground-water withdrawal from unconsolidated sediment. In: Man-induced Land Subsidence (ed. by T. L. Holzer), *Geol. Soc. Am., Reviews in Engineering Geology* **6**, 67–105.

Holzer, T. L. (2000) Methods for prediction of earth fissures and faults associated with groundwater withdrawal. In: *The Fragile Territory*, 10th Congresso Nazionale dei Geologi, Consiglio Nazionale dei Geologi, Rome, 179–185.

Holzer, T. L., Davis, S. N. & Lofgren, B. E. (1978) Faulting caused by groundwater extraction in southcentral Arizona. *J. Geophys. Res*. **84**(B2), 603–612.

Holzer, T. L. & Pampeyan, E. H. (1981) Earth fissures and localized differential subsidence. *Water Resour. Res.* **17**(1), 223–227.

Jachens, R. C. & Holzer, T. L. (1982) Differential compaction mechanism for earth fissures near Casa Grande, Arizona, *Bull. Geol. Soc. Am.* **93**(10), 998–1012.

Lee, K. L. & Shen, C. K. (1969) Horizontal movements related to subsidence. *ASCE J. Soil Mechanics* **94**(SM6), 140–166.

Leonard, R. J. (1929) An earth fissure in southern Arizona. *J. Geology* **37**(8), 765–774.

Lofgren, B. E. (1969) Land subsidence due to the application of water. In: (ed. by D.J. Varnes and G. Kiersch) *Geol. Soc. Am. Reviews in Engineering Geology* **2**, 271–303.

Lofgren, B. E. (1971) Significant role of seepage stresses in compressible aquifer systems (abstract). *Eos, Trans. AGU* **52**(11), p. 832.

Lofgren, B. E. (1978) Hydraulic stresses cause ground movement and fissures, Picacho, Arizona. *Geol. Soc. Am. Abstracts with Programs* **10**(3), p. 113.

Lufkin (1972) *Taping Techniques for Engineers and Surveyors*. The Lietz Company, Carson, California, USA.

Maxey, G. B. & Jameson, C. H. (1948) Geology and water resources of Las Vegas, Pahrump, and Indian Spring Valleys, Clark and Nye Counties, Nevada. *Nevada Water Resources Bulletin* **5**, p. 121.

Neal, J. T., Langer, A. M. & Kerr, P. F. (1968) Giant desiccation polygons of Great Basin playas. *Bull. Geol. Soc. Am.* **79**(1), 69–90.

Pampeyan, E. H., Holzer, T. L. & Clark, M. M. (1988) Modern ground failure in the Garlock fault zone, Fremont Valley, California. *Bull. Geol. Soc. Am.* **100**(5), 677–691.

Pankratz, L. W., Ackermann, H. D. & Jachens, R. C. (1978) Results and interpretation of geophysical studies near the Picacho Fault, south-central Arizona. *US Geological Survey Open-file Report 78-1106*, p. 17.

Peterson, D. E. (1962) Earth fissuring in the Picacho area, Pinal County, Arizona. Department of Geology, University of Arizona, Tucson.

Schumann, H. H. (1974) Land subsidence and earth fissures in alluvial deposits in the Phoenix area, Arizona. *US Geological Survey, Miscellaneous Investigations Map I-845-H*.

Sheng, Z., Helm, D. C. & Li, J. (2003) Mechanisms of earth fissuring caused by groundwater withdrawal. *Environ. Engng Geoscience* **9**(4), 351–362.